International Journal of Biological Macromolecules 291 (2025) 139084

Contents lists available at ScienceDirect

International Journal of Biological Macromolecules

journal homepage: www.elsevier.com/locate/ijbiomac

Glycogenin is dispensable for normal liver glycogen metabolism and body glucose homeostasis

Xinle Tan [a], Giorgia Testoni [b], Mitchell A. Sullivan [c,d], Iliana López-Soldado [b], Francisco Vilaplana [e], Robert G. Gilbert [f,g,*], Joan J. Guinovart [b], Benjamin L. Schulz [h], Jordi Duran [i,j]

[a] Centre for Animal Science and Centre for Nutrition and Food Science, Queensland Alliance for Agriculture and Food Innovation, The University of Queensland, Brisbane, Queensland 4072, Australia
[b] Institute for Research in Biomedicine of Barcelona (IRB Barcelona), The Barcelona Institute of Science and Technology, Barcelona 08028, Spain
[c] School of Health, University of the Sunshine Coast, Sippy Downs, Queensland 4556, Australia
[d] Mater Research Institute—The University of Queensland, Translational Research Institute, Brisbane, Queensland 4102, Australia
[e] Division of Glycoscience, Department of Chemistry, KTH Royal Institute of Technology, AlbaNova University Centre, 106 91, Stockholm, Sweden
[f] Jiangsu Key Laboratory of Crop Genomics and Molecular Breeding/Key Laboratory of Plant Functional Genomics of the Ministry of Education, and Jiangsu Key Laboratory of Crop Genetics and Physiology, Agricultural College of Yangzhou University/Jiangsu Co-Innovation Centre for Modern Production Technology of Grain Crops, Yangzhou University, Yangzhou, Jiangsu Province 225009, China
[g] Centre for Nutrition and Food Science, Queensland Alliance for Agriculture and Food Innovation, The University of Queensland, Brisbane, Queensland 4072, Australia
[h] School of Chemistry and Molecular Biosciences, The University of Queensland, Brisbane, Queensland 4072, Australia
[i] Institut Químic de Sarrià (IQS), Universitat Ramon Llull (URL), Barcelona 08017, Spain
[j] Institute for Bioengineering of Catalonia (IBEC), The Barcelona Institute of Science and Technology, Barcelona 08028, Spain

ARTICLE INFO

Keywords:
Glycogen
Glycogenin
Glucose metabolism
Glycogen α particles
Liver

ABSTRACT

Glycogen is a glucose-storage polysaccharide molecule present in animals, fungi and bacteria. The enzyme glycogenin can self-glycosylate, forming an oligosaccharide chain that primes glycogen synthesis. This priming role of glycogenin was first believed to be essential for glycogen synthesis, but glycogen was then found in the skeletal muscle, heart, liver and brain of glycogenin-knockout mice (Gyg KO), thereby showing that glycogen can be synthesized without glycogenin. Within the liver, glycogen is present in the form of individual glycogen particles, called β particles, and larger composite aggregates of linked β particles, called α particles. Previous studies suggested that liver glycogenin plays a role in linking β particles into α particles and thus participating in glucose homeostasis, which implies that α particles would be absent in Gyg KO mice liver. Here we test this through targeted characterization of glycogen structure and through proteomic and metabolic studies on Gyg KO mice. The results show that, contrary to what had been believed, glycogenin is not necessary for normal liver-glycogen metabolism.

1. Introduction

Most living organisms use glucose as their primary energy source for metabolism. Glycogen is a highly branched polysaccharide that serves as a glucose storage molecule in animals [1], fungi [2] and bacteria [3]. Given the key role of glycogen in metabolism, evolutionary forces ensure that these organisms have developed a means of synthesizing this molecule, although the biosynthetic process may not be the same across species; because glycogen is essential for these various species, it would not be surprising if more than one pathway had evolved for its biosynthesis in different organisms (indeed, such redundancy is not uncommon in nature [4]). Here we examine certain biosynthetic aspects of the protein glycogenin, a molecule involved in glycogenesis in all species examined to date.

Glycogen biosynthesis in mammals starts with an oligosaccharide chain primed by glycogenin [5,6], which is then elongated by glycogen synthase (GS, which adds glucose via (1 → 4)-α glycosidic linkages), and by glycogen branching enzyme (GBE), which introduces branches via (1

* Corresponding author at: Centre for Nutrition and Food Science, Queensland Alliance for Agriculture and Food Innovation, The University of Queensland, Brisbane, Queensland 4072, Australia.
E-mail address: b.gilbert@uq.edu.au (R.G. Gilbert).

https://doi.org/10.1016/j.ijbiomac.2024.139084
Received 4 November 2024; Received in revised form 8 December 2024; Accepted 20 December 2024
Available online 21 December 2024

→ 6)-α linkages. In most mammals, glycogenin is present in two isoforms: GYG1, which is widely expressed, and GYG2, which is predominantly found in the liver. However, rodents carry a single glycogenin gene (*Gyg1*), which is expressed in all tissues [7,8]. Glycogenin can self-glycosylate to form a chain of around 10 anhydroglucose units attached to a tyrosine residue, which then provides a primer for glycogen synthesis [9]. This priming role of glycogenin had been believed to be essential for glycogen synthesis. However, we previously showed that glycogenin-knockout mice (Gyg KO) synthesize glycogen in all tissues analyzed, namely skeletal muscle, cardiac muscle, brain and liver [10], despite the lack of glycogenin. Other researchers reported that lack of glycogenin-1 did not affect human muscle glycogen synthesis [11]. Liver and brain glycogen were found to be present at normal levels in Gyg KO mice, while glycogen content in skeletal muscle even increased, which in turn caused a switch of oxidative myofibers towards glycolytic metabolism [10]. More recently, we demonstrated that the lack of glycogenin impairs pulmonary glycogen metabolism, resulting in respiratory distress syndrome [12]. Similar results were found in humans: lack of glycogenin lead to abnormal glycogen storage in the heart [11]. Thus, in some tissues, although glycogen is still present, the lack of glycogenin results in functional disturbances.

Glycogen is present in the liver in the form of compound particles. Small β particles, ~20 nm in diameter and comprising randomly-branched anhydroglucose monomer units [13], are joined together to form large α particles with a diameter up to 300 nm [14]. This wide size range contributes to improved regulation of glucose release, as larger particles degrade more slowly when exposed to glycogen phosphorylase [15]. Therefore, α particles are important in the maintenance of blood-glucose homeostasis [16] and α particle structure integrity was found associated with the development of diabetes [15–17]. Glycogenin has been proposed to be the protein that binds β particles together to form α particles [18]. Although glycogen levels are normal in the livers of Gyg KO mice [10], the synthesis and degradation of liver glycogen in the absence of glycogenin might have different kinetics than that of glycogen primed by glycogenin, and might thus have an effect on whole-body glucose homeostasis. Here we test the hypothesis that the absence of glycogenin in mouse liver will lead to the absence of glycogen α particles and thus impact liver metabolism in general.

The investigation of the above hypothesis can help to clarify some current knowledge gaps, including the following. 1) Glycogenin depletion leads to multiple functional disturbances; the effects of this depletion on the structure of glycogen α particles, and how such depletion might affect glycogen metabolism, are not well understood. 2) The effects of glycogenin knock-out on liver metabolism (the liver being the main glycogen storage organ) merit deeper exploration. Addressing these gaps is important in refining knowledge of the mechanisms underlying glycogen metabolism and the involvement of glycogenin in its regulation.

Here we explore the role of glycogenin in the liver by: 1) employing a SWATH (Sequential Window Acquisition of all THeoretical fragment ion spectra mass spectrometry) proteomic investigation and analyzing glucose body homeostasis to study liver glycogenin function in vivo; and 2) characterizing the structure of glycogen to test the hypothesis that glycogenin is essential for the formation of α particles. Our results show, somewhat to our surprise, that glycogenin is largely dispensable for normal glycogen metabolism in the liver and for the regulation of glycaemia.

2. Methods

2.1. Animals

Gyg KO mice were generated as previously described (see [10] for detailed genotype information). Briefly, ES cells ($Gyg^{tm1a(KOMP)Wtsi}$) were obtained from the KOMP Repository (www.komp.org). Mice heterozygous for the glycogenin (Gyg) gene were obtained from ES cells in a C57Bl6 background and subsequently bred to produce Gyg KO animals. Mice were kept in the Barcelona Science Park Animal Facility (Spain) in specialized pathogen-free conditions, under a 12 h light-dark cycle and, unless indicated, they had unlimited access to food and water. All experimental protocols were approved by the Barcelona Science Park Animal Experimentation Committee and were carried out following Spanish (BOE 34/11370–421, 2013) and European Union (2010/63/EU) regulations and the National Institutes of Health guidelines for the care and use of laboratory animals. Experiments were conducted using litter mates, and unless indicated, males and females were included in each group. Where necessary, groups included multiple litters for statistical validity. The design of specific genotyping probes and genotyping was performed using TransnetYX^{R}. The genotype of the knockout mice were confirmed by western blot analysis in our previous publication [10].

In the production of knockout mice, it is important to note that most embryos were still-born or died shortly after birth. This observation thus indicates the importance of adequate glycogenin production for reproductive health. The mice were then subjected to following experiments as shown in Fig. 1.

2.2. Treadmill exercise

Treadmill exercises were performed as previously described [10]. Briefly, mice were accustomed to running on a treadmill (Columbus Instruments) for 5 min a day for 5 days at a speed of 10 to 14 cm/s and on a 0° slope. On the day of the trial, animals ran for 3 min on a treadmill with a 10° slope and at a speed of 10 cm/s. The pace was increased by 2 cm/s every 2 min until the mice were exhausted or a maximum speed of 46 cm/s was reached. Mice were then sacrificed, and the liver was quickly removed and frozen in liquid nitrogen.

2.3. Glucose tolerance test, insulin tolerance test, and glucagon tolerance test

A glucose tolerance test (GTT) was performed as previously described [19]. Briefly, 2 g/kg (body weight) of glucose was administered intraperitoneally to mice after an overnight fast (16 h). A glucometer (Contour Next, Bayer Healthcare) was used to measure glycaemia in tail blood taken at the indicated times after injection. An insulin tolerance test (ITT) was performed in 6-h fasted mice after an intraperitoneal injection of 0.75 units/kg of insulin. Blood glucose was measured at the indicated time points after the challenge. A glucagon tolerance test was performed in 6-h fasted mice after an intraperitoneal injection of 100 μg/kg of glucagon. Blood glucose was measured at the indicated time points after the challenge.

2.4. Blood and biochemical analysis

Glycogen content was determined in samples of the frozen liver by measuring amyloglucosidase-released glucose from glycogen, as previously described [20]. GS activity was determined in the presence or absence of glucose-6-phosphate (G6P), as previously described [21]. GS activity measured in the presence of saturating G6P [(+) G6P] corresponds to the total amount of enzyme, whereas measurement in its absence [(−) G6P] is an indication of the active (unphosphorylated) GS form. The (−) G6P / (+) G6P activity ratio is an estimate of the activity state of the enzyme. GP activity was determined by measuring the incorporation of [U-^{14}C] glucose from [U—^{14}C] glucose-1-phosphate into glycogen in the presence of 5 mmol/L AMP [22]. ATP, AMP, and ADP were measured from perchloric acid extracts of the liver, as previously described [23], using a Brisa LC2 C18 column (4.6 mm × 150 mm, 3 μm particle size) interfaced with a photodiode array detector (260 nm) and a constant flow rate of 0.6 mL/min. Liver lactate was measured in perchloric-acid extracts, as previously described [24–26]. The intracellular concentration of G6P was measured in perchloric-acid

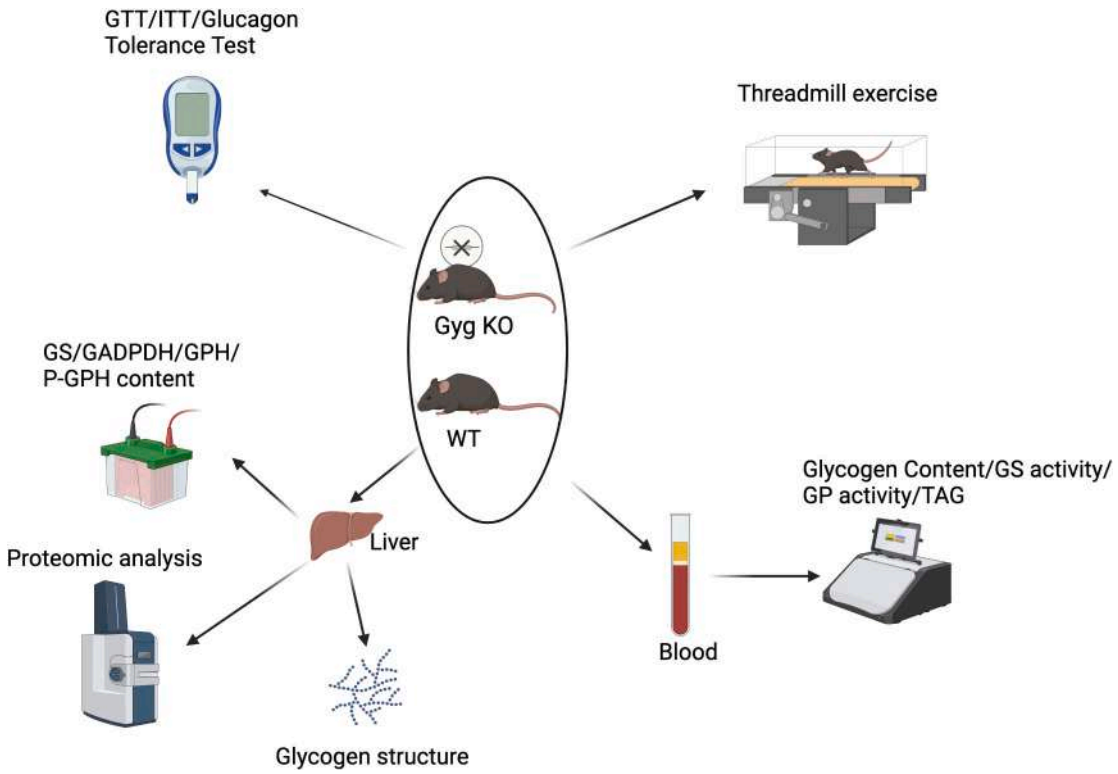

Fig. 1. Schematic of research protocol. Created in BioRender. Tan, X. (2024) https://BioRender.com/x42u085

extracts with a fluorometric assay, as described in [27]. Hepatic triacylglycerol (TAG) was quantified in 3 mol/L KOH and 65 % ethanol extracts, following the method described by Salmon and Flatt [28] using a kit (Sigma-Aldrich, St Louis, MO, USA).

2.5. Western blot analyses

Liver samples were homogenized in 50 mM Tris/HCl (pH 7.4), 150 mM NaCl, 1 mM EDTA, 5 mM sodium pyrophosphate, 1 mM sodium orthovanadate, 50 mM NaF, 1 % NP-40, 1 mM PMSF, and a protease inhibitor cocktail tablet (Roche) [25]. Homogenates were agitated for 1 h at 4 °C in an orbital shaker and centrifuged at 16,000*g* for 15 min at 4 °C. Proteins were resolved in 10 % acrylamide gels for SDS-PAGE and transferred to Immobilon membranes (Millipore). Immunoblot analysis of homogenates was performed using the following antibodies: GS (ref. 3886 from Cell Signaling), GAPDH (ref. AM4300 from Thermo Fisher Scientific), GPH (Rabbit, peptide 830–850, Genosys), and P-GPH (IgY, Chicken, phosphopeptide 9–19, Genosys).

2.6. Statistical methods

In Figs. 3–8, the data are expressed as the mean ± SEM. Significance between the groups was analyzed with Prism8 software (GraphPad) using a Student's *t*-test, or ANOVA with post hoc Tukey tests, as appropriate. The following *p* values were considered to be statistically significant: p value <0.05 (*), p value <0.01 (**), and p value <0.001(***).

2.7. Whole liver sample preparation for proteomic analysis

Liver tissue was homogenized, denatured, and reduced or alkylated as previously described [29], with minor changes. Briefly, approximately 50 mg of liver tissue was mixed with guanidine denaturing buffer (6 M guanidinium, 10 mM DTT, and 50 mM Tris-HCl) to a final volume of 1 mL and then homogenized with a Dounce homogenizer and centrifuged at 1500*g* for 5 min. The supernatants were transferred to new tubes, and cysteines were alkylated by the addition of acrylamide to a final concentration of 30 mM, and then incubation at 30 °C for 1 h with shaking. The excess acrylamide was then removed by the addition of DTT to a final concentration of 10 mM. Samples were clarified by centrifugation at 18,000*g* for 10 min at room temperature. The supernatants were collected and processed with Filter Assisted Sample Preparation (FASP) [29] using a 10 kDa cutoff Amicon ultra 0.5 mL filter (EMD Millipore, Billerica, MA) by centrifugation at 14,000*g* for 20 min at room temperature. A volume of 200 μL of 50 mM ammonium acetate was added to the filters, and samples were further centrifuged at 14,000*g* for 20 min and diluted with 130 μL of 50 mM ammonium acetate. Trypsin (proteomics grade, Sigma) was added in a 1:100 (enzyme/protein) ratio, and the mixture was incubated overnight at 37 °C with shaking. The trypsin-digested peptides were then eluted by centrifugation at 14,000*g* for 20 min. Columns were washed with 50 μL of 0.5 M NaCl and centrifuged at 14,000*g* for 20 min. Trypsin-digested peptides were desalted with C18 ZipTips (Millipore) following the manufacturer's instructions. A pooled sample with approximately 40 μg of peptides in a total volume of 500 μL 0.1 % formic acid solution was subjected to high pH reverse-phase fractionation. Peptides were added to a 50 mg tC18 Sep-Pak (Waters), washed with 500 μL of double distilled water, eluted in eight separate 500 μL fractions of acetonitrile (5 %, 7.5 %, 10 %, 12.5 %, 15 %, 17.5 %, 20 %, and 50 %) in 0.1 % triethylamine, vacuum-dried (miVac Centrifugal Concentrators, Genevac, UK), and resuspended in 0.1 % formic acid.

2.8. Mass spectrometry

An LC-ESI-MS/MS setup, using a Prominence nanoLC system (Shimadzu) and a TripleTof 5600 instrument with a Nanospray III interface (SCIEX), was used to obtain MS/MS spectral data, as previously described [30]. For the whole-liver extract library construction, 50 μL samples of each desalted fraction from the previous section were injected for data-dependent acquisition (DDA). For data-independent acquisition (DIA), 8 μL (~0.4 μg peptides) was injected for SWATH

analysis. LC parameters were identical for DDA and DIA, and LC-MS/MS was performed as previously described [30]. Peptides were separated with buffer A (1 % acetonitrile and 0.1 % formic acid) and buffer B (80 % acetonitrile with 0.1 % formic acid) in a gradient of 10–60 % buffer B over 45 min, for a total run time of 70 min per sample. Gas and voltage settings were adjusted as required. For DDA analyses, an MS-TOF scan from *m/z* of 350–1800 was performed for 0.5 s, followed by DDA of MS/MS in high-sensitivity mode with automated CE selection of the top 20 peptides from *m/z* of 40–1800 for 0.05 s per spectrum and dynamic exclusion of peptides for 5 s after 2 selections. Identical LC conditions were used for DIA SWATH, with an MS-TOF scan from an *m/z* of 350–1800 for 0.05 s followed by high-sensitivity DIA of MS/MS from *m/z* of 50–1800 with 26 *m/z* isolation windows with 1 *m/z* window overlap each for 0.1 s across an *m/z* range of 400–1250. Collision energy was automatically assigned by Analyst software (SCIEX) based on *m/z* window ranges.

2.9. Data analysis

Peptide identification was performed essentially as previously described [30] using ProteinPilot 5.0.1 (SCIEX), searching against the *Mus musculus* (Mouse) proteome with standard settings: sample type, identification; cysteine alkylation, acrylamide; instrument, TripleTof 5600; species *Mus musculus*; ID focus, biological modifications; enzyme, trypsin; Search effort, thorough ID. False discovery rate analysis using ProteinPilot was performed on all searches with limits of 99 % identification confidence and 1 % local false discovery rate. The ProteinPilot search results were used as ion libraries for SWATH analyses. Peptide abundance was measured using PeakView software with standard settings, summing the integrated areas of up to six fragment ions per peptide. Protein abundance was measured using the sum of the abundances of up to six peptides per protein. Protein-centric analyses were performed as previously described [31], and protein abundances were recalculated using a strict 1 % FDR cutoff [32]. Normalization was performed to the total protein abundance in each sample, as previously described [33]. Principal component analysis (PCA) was performed using R (version 4.3.2). The heatmap was generated with Pheatmap package (version 1.0.12) from R (version 4.3.2). Statistical analyses for SWATH proteomics were performed using MSstats in R [30]. PeakView output was reformatted as previously described [32] and significant differences in protein abundance were determined using MSstats (2.4) [34] in R, with a significance threshold of $p = 10–5$ [35]. Gene ontology (GO) term enrichment was performed using GOstats (2.39.1) [36] in R, with a significance threshold of $p = 0.05$ [35]. The mass spectrometry proteomics data have been deposited to the ProteomeXchange Consortium via the PRIDE [37] partner repository with the dataset identifier PXD054512. Reviewer account details: Username: reviewer_pxd054512@ebi.ac.uk. Password: t0jvWX55x1RC.

2.10. Degradation of glycogen by acid

A method similar to that used previously [38] was employed for the acid hydrolysis of liver glycogen. Glycogen samples (6 from WT (wild-type) and 5 from Gyg KO mouse models) were dissolved in 0.1 M sodium acetate buffer (2 mg/mL, pH ~3.5) and heated to 80 °C in a thermomixer for timed intervals between 30 min and 18 h. The samples were removed from the thermomixer at 30 min, 1 h, 2 h and 18 h, and precipitated with four volumes of ethanol. Glycogen pellets were collected by centrifugation at 4000*g* for 10 min and then dissolved in aqueous ammonium nitrate eluent (50 mM NH_4NO_3 with 0.02 % sodium azide) for SEC and FACE analyses.

2.11. Size-exclusion chromatography (SEC)

SEC was performed with a water-based eluent. Glycogen samples obtained as described above were dissolved in 200 μL eluent solution (50 mM NH_4NO_3 with 0.02 % sodium azide). This was followed by injection of the liver glycogen samples into an Prominence LC-20 CE SEC (Shimadzu) with SUPREMA pre-column and with 1000 and 10,000 columns (Polymer Standards Service, Mainz, Germany) in series [39]. An oven was used to keep columns at 80 °C with the flow rate 0.3 mL/min [39]. A refractive index detector (Optilab UT-rEX, WYATT, Santa Barbara, CA, USA) was connected to the column outlet to give the SEC weight distribution as a function of the hydrodynamic radius of the analyte, w ($\log R_h$) [39]. Pullulan standards (PSS) with a molar mass range of 342–2.35 × 10^6 Da were used for the universal calibration curve; these were dissolved in the same SEC eluent (50 mM ammonium nitrate/0.02 % sodium azide) as that used for the samples. The glycogen weight distribution was normalized to the highest peak between R_h = 0–60 nm.

For statistical analysis of the β particle ratio (BetaRatio), glycogen particles with $R_h < 30$ nm were defined as β particles and those in the range 30 nm < R_h < 60 nm as α particles. The Areas Under the Curves (AUC) of α and β particles were integrated and the BetaRatio was defined as:

$$\text{BetaRatio} = \text{AUC}\beta \,/\, (\text{AUC}\beta + \text{AUC}\alpha)$$

2.12. Chain length distributions

Glycogen samples were debranched as previously described [40]; 0.9 mL of deionized water was added to glycogen (1–2 mg) samples for heating at 100 °C for 10 min before cooling to room temperature. Next, 0.1 mL of sodium acetate buffer (pH 3.5) and 2.5 μL of isoamylase (1000 U/mL) were added to the samples, which were then vortexed and incubated at 37 °C for 30 min. The pH of the samples was adjusted to 7 with ~0.1 mL of sodium hydroxide (0.1 M) and samples were then heated at 80 °C for 1 h. These debranched samples were then frozen in liquid nitrogen and lyophilized (VirTis BTP-9EL freeze-dryer). Debranched glycogen chains (0.2 mg) were labelled with APTS (8-amino-1,3,6-pyrenetrisulfonic acid) in 2 mL Eppendorf tubes by adding 1.5 μL of a solution of APTS (0.1 mg μL^{-1}) in 15 % glacial acetic acid and 1.5 μL of 1 M aqueous sodium cyanoborohydride. The reaction mixture was vortexed and incubated at 60 °C for 1.5 h in the dark, diluted with 80 μL of Milli Q water and vortexed until all the precipitate dissolved. The insoluble material was removed by centrifugation at 4000*g* for 10 min, and 50 μL of the supernatant was then transferred to 200 μL microcentrifuge tubes for immediate fluorophore-assisted carbohydrate electrophoresis (FACE) analysis.

The CLDs (chain length distributions) were obtained using FACE. Labelled chains were separated on a PA-800 Plus System and quantified with a solid-state laser-induced fluorescence (LIF) detector with an argon-ion laser as the excitation source (Beckman-Coulter, Brea, CA, USA). A 50-μm diameter NCHO-coated capillary (included in the Carbohydrate Labeling and Analysis Kit) was used to separate samples. Carbohydrate separation buffer, also included in the kit, was used as the separating medium. The sample was injected into the capillary for 3 s at 0.5 psi (3.4 kPa above atmospheric pressure). Separation of the labelled linear glucans was achieved using an applied voltage of 30 kV at 25 °C.

3. Results

3.1. SWATH analysis of whole liver extract

To study the consequences of the lack of glycogenin in the liver, we first profiled proteomes from whole-liver extracts from Gyg KO and WT mice. A total of 750 proteins were identified with a false discovery rate (FDR) of <1 %. Of these, 612 were quantified by sequential window acquisition of all theoretical fragment ion spectra mass spectrometry (SWATH). Based on this successfully quantified protein list, the protein abundance information was subjected to principal component analysis (PCA). Clusters of liver samples from WT (black) and Gyg KO mice (red) overlapped, and the separation between the groups was not obvious

from the PC1 and PC2 coordinates (Fig. 2A). Specifically, WT samples were clustered in the centre while the Gyg KO samples were scattered. This pattern is consistent with clusters in the heatmap (Fig. 2C), where Gyg KO and WT samples were not completely separated based on relative protein abundance but still showed close distance among most samples from the same genetic background: WT6, KO2, WT5, WT1, WT7, WT2, WT8, and WT4 showed close relationship in the phylogenetic analysis and the rest of the samples were relatively distant.

To explore the specific differences in the whole liver extract proteome, MSstats analysis combined with GO term enrichment analysis was applied to the differentially abundant proteins. Five proteins were found to be increased in abundance and 6 proteins decreased in Gyg KO mice with a $p < 0.00001$ and $|\log2FC| > 0.5$ cut-off (Table 1). These differentially abundant proteins were visualized by a volcano plot in (Fig. 2B). GO term enrichment analysis of the differentially abundant proteins did not generate significantly enriched terms from either the increased or decreased protein list. Close inspection of the MSstats result showed that proteins relating to fatty acid synthesis or ATP production (UDP-glucuronosyltransferase 1A1) were significantly different. Other significantly different proteins were common in cytoplasm or membrane (glutathione S-transferase Mu 6, indolethylamine *N*-methyltransferase, indolethylamine *N*-methyltransferase, histone H3.2, cathepsin B), mitochondria (ATP-citrate synthase, D-lactate dehydrogenase) possibly comtamination (keratin, type II cytoskeleal 75). However, as no GO terms were significantly enriched from the differentially abundant protein list, these differences were minor.

3.2. Liver glycogen content

The amount of glycogen stored in the liver is regulated by the balance between glycogen synthesis and glycogen degradation. We previously showed that the consequences of the absence of glycogenin in glycogen content are tissue-specific: Gyg KO mice were found to accumulate significantly more glycogen in muscle and heart, whereas they showed normal glycogen levels in liver and brain [10]. To find possible subtle differences, we further refined the measurement of glycogen levels in the livers of Gyg KO mice. Liver glycogen content did not show significant differences across age and gender subgroups (Fig. 3A, and B). To analyze liver glycogen mobilization, glycogen content was also measured after extenuating exercise. Both groups showed a significant decrease in liver glycogen after exercise, but no difference was observed between Gyg KO and WT mice (Fig. 3C).

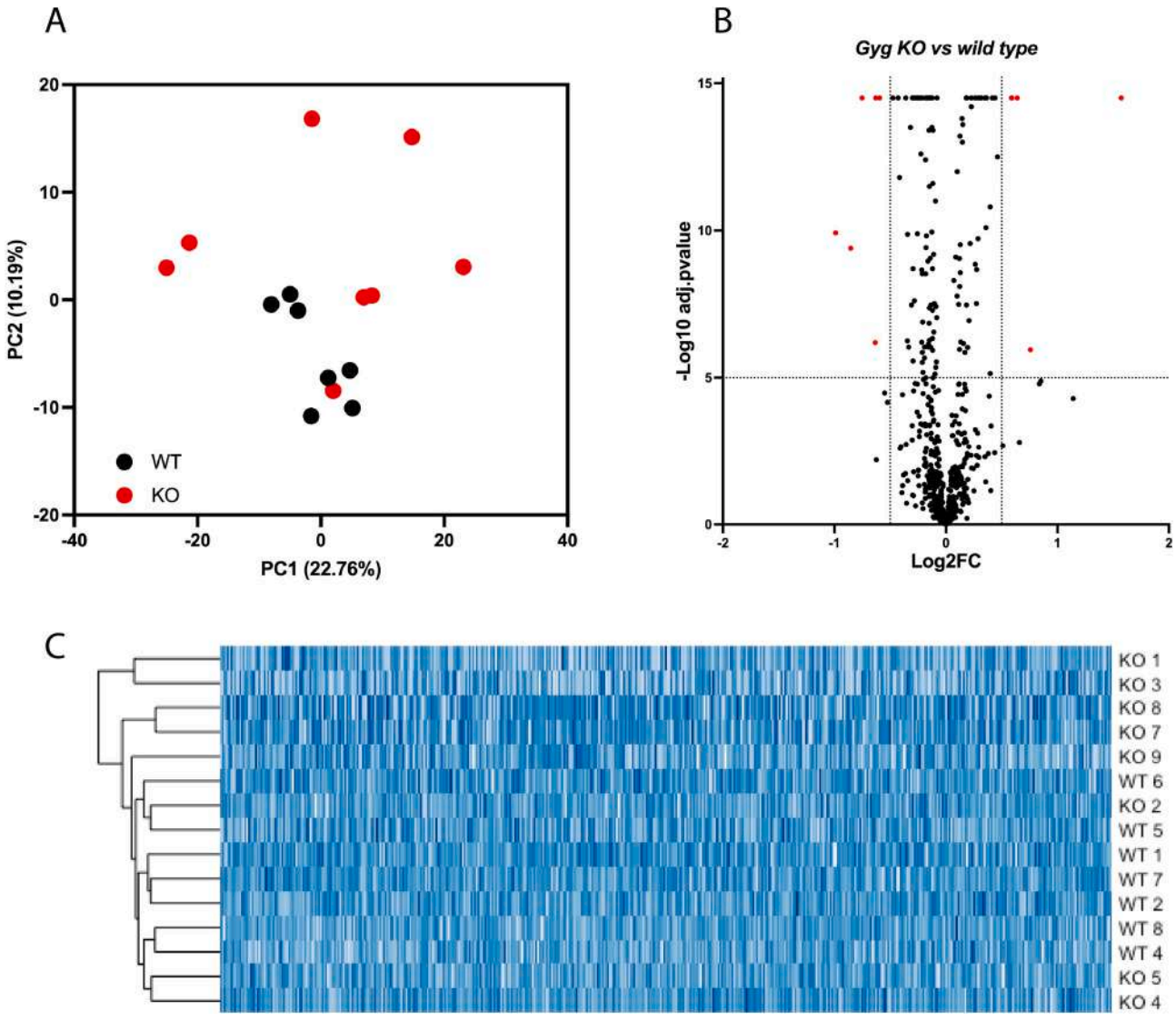

Fig. 2. Mouse liver proteome characterization. A, Principle Component Analysis of WT and Gyg KO mouse-liver proteome. B, Volcano plot of Gyg KO vs. WT proteins. C, Heatmap of WT and Gyg KO proteome. (A), Proteins with adj.pvalue of 0 were set to the next lowest value (−log10(adj. pvalue) = 14.5) for display purposes.

Table 1
Differentially abundant proteins from Gyg KO mice compared to WT mice.

Protein	log 2FC	Adj. p value	Protein name
Upregulated			
sp|P19096|FAS_MOUSE	0.587581	3.40×10^{-15}	Fatty acid synthase
sp|Q05816|FABP5_MOUSE	0.638704	3.40×10^{-15}	Fatty acid binding protein 5
sp|Q8BGZ7|K275_MOUSE	1.572474	3.40×10^{-15}	Keratin, type II cytoskeleal 75
sp|Q91V92|ACLY_MOUSE	0.590458	3.40×10^{-15}	ATP-citrate synthase
sp|O35660|QSTM6_MOUSE	0.757191	1.12×10^{-6}	Glutathione S-transferase Mu 6
Downregulated			
sp|P40939|INMT_MOUSE	−0.629435	3.40×10^{-15}	Indolethylamine *N*-methyltransferase
sp|Q63886|UD11_MOUSE	−595,274	3.40×10^{-15}	UDP-glucuronosyltransferase 1A1
sp|Q64459|CP3AB_MOUSE	−0.752391	3.40×10^{-15}	Cytochrome P450 3 A11
sp|Q7TNG8|LDHD_MOUSE	−0.989169	1.20×10^{-10}	Probable D-lactate dehydrogenase, mitocondrial
spP84228|H32_MOUSE	−0.85411	3.97×10^{-10}	Histone H3.2
sp|P10605|CATB_MOUSE	−0.633769	6.53×10^{-7}	Cathepsin B

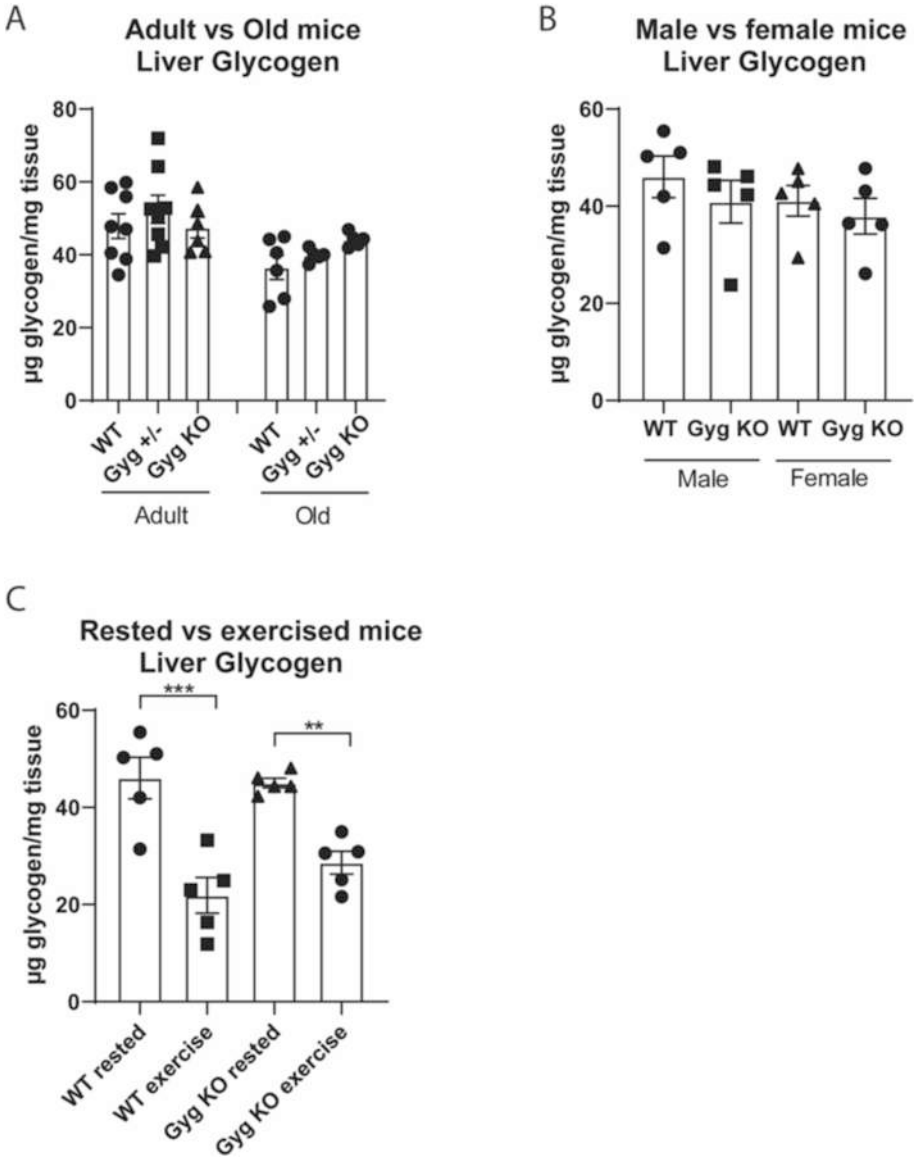

Fig. 3. Characterization of liver glycogen content. A) Biochemical quantification of glycogen content in the livers of adult (18 weeks old) and old (60 weeks old) WT, heterozygous (Gyg +/−) and Gyg KO mice, $n = 5$–8 per group. B) Biochemical quantification of glycogen content in livers of male and female mice, n = 5 per group. C) Biochemical quantification of glycogen content in liver of rested and exercised mice, n = 5 per group; $^{**}p < 0.01$, $^{***}p < 0.001$.

3.3. Glycogen molecular size distribution

Based on a previous report that glycogenin is involved in the regulation of the higher-order structure of liver glycogen [18],here we tested whether glycogen structure was altered in Gyg KO mouse liver. To this end, we characterized the structure of this molecule by obtaining glycogen size distributions (the distribution of the relative total weight of molecules as a function of their molecular size in the solvent) from size exclusion chromatography (SEC), and chain length distributions from fluorophore-assisted carbohydrate electrophoresis (FACE). The results show that glycogen from fasted WT and Gyg KO mouse livers was mainly composed of α particles regardless of whether the animals were fasted or reinjected with glucose (Fig. 4). The observation that α particles still formed even when Gyg was knocked out indicates that glycogenin is not essential for α-particle formation, which disproves the hypothesis [18] that glycogenin is the only linking agent between β particles to form α particles. Furthermore, there were no significant differences in the chain length distributions between the liver glycogen of Gyg KO (red) and WT (wild-type) mice (blue) (Fig. 5), which characterized the individual glucose polymer chain length when higher-level structure (α and β particles) was disrupted. This chain length distribution is associated with relative enzyme activities involving in glycogen synthesis [41].

3.4. WT and Gyg KO liver glycogen show the same acid-degradation pattern

To further explore possible differences in α-particle structure between the two groups, we designed experiments to characterize α-particle degradation patterns under acidic conditions. In these conditions, glycogen α particles tend to disintegrate preferentially into β particles before degrading into glucose molecules, while in phytoglycogen, a protein-free glycogen model, no individual β particles are observed during acid degradation [38]. If glycogenin participates in linking β particles into α particles, we expected the acid-degradation pattern of Gyg KO liver glycogen to differ from that of WT, perhaps similar to that of phytoglycogen. At pH = 3.5, WT mouse-liver glycogen α particles

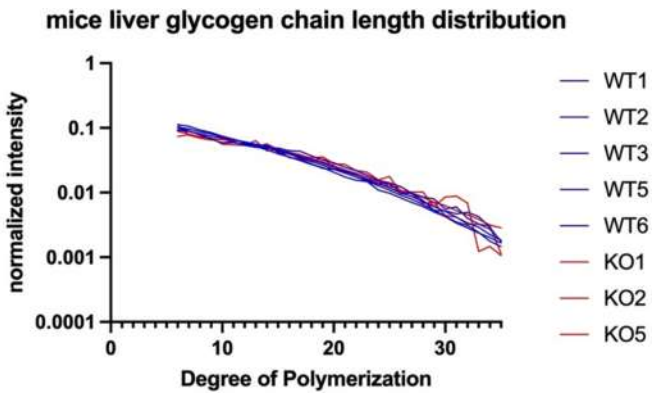

Fig. 5. Chain-length distribution of glycogen from livers of WT (blue) and Gyg KO mice (red). (For interpretation of the references to colour in this figure legend, the reader is referred to the web version of this article.)

were degraded into smaller particles, as expected, and these smaller particles were dominant after 18 h of incubation (Fig. 5). When Gyg KO mouse-liver glycogen was subjected to identical conditions, the same degradation pattern was observed: α particles first degraded to β particles under acid incubation, showing a two-phase degradation pattern (α particles degraded to β particles and then to glucose molecules). SEC size distributions did not show any obvious differences between glycogen from the two groups of mice (Fig. 6). These results again indicate that glycogenin is dispensable for the normal formation of α particles.

3.5. Enzymatic activities and energy state

Glycogen-related metabolic processes include GS catalysis of the addition of glucose units to existing polysaccharide molecules, and GP catalysis of the removal of glucose monomers from glycogen. We measured liver GS activity in the presence of saturating G6P (+G6P), corresponding to the total amount of enzyme, and in its absence (–G6P), as an indication of the active (unphosphorylated) GS form, as well as GP

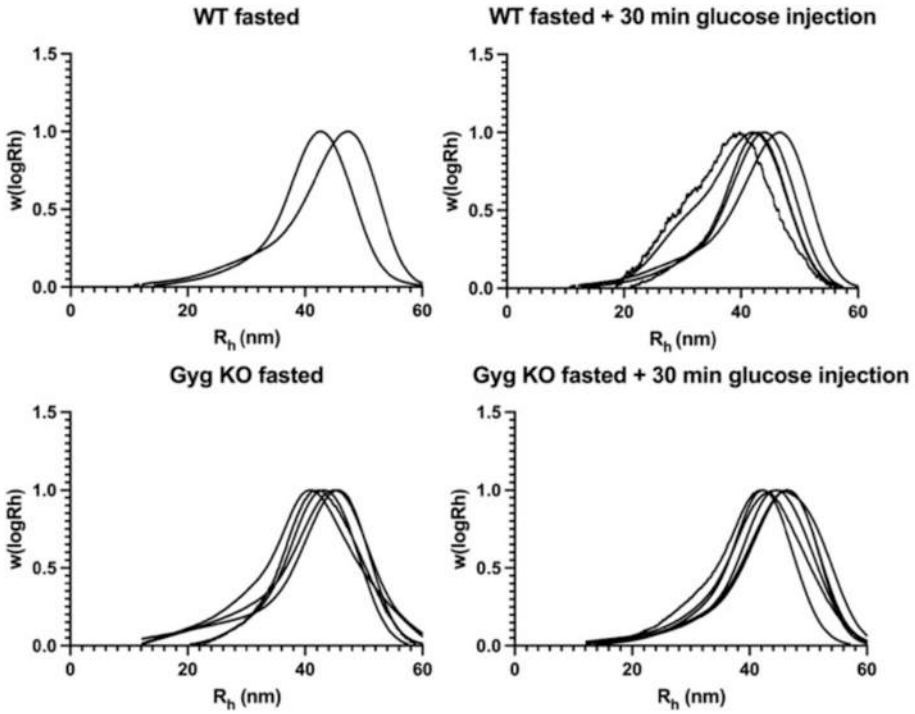

Fig. 4. Glycogen weight distribution in livers of fasted WT and Gyg KO mice and 30 min after glucose injection treatment.

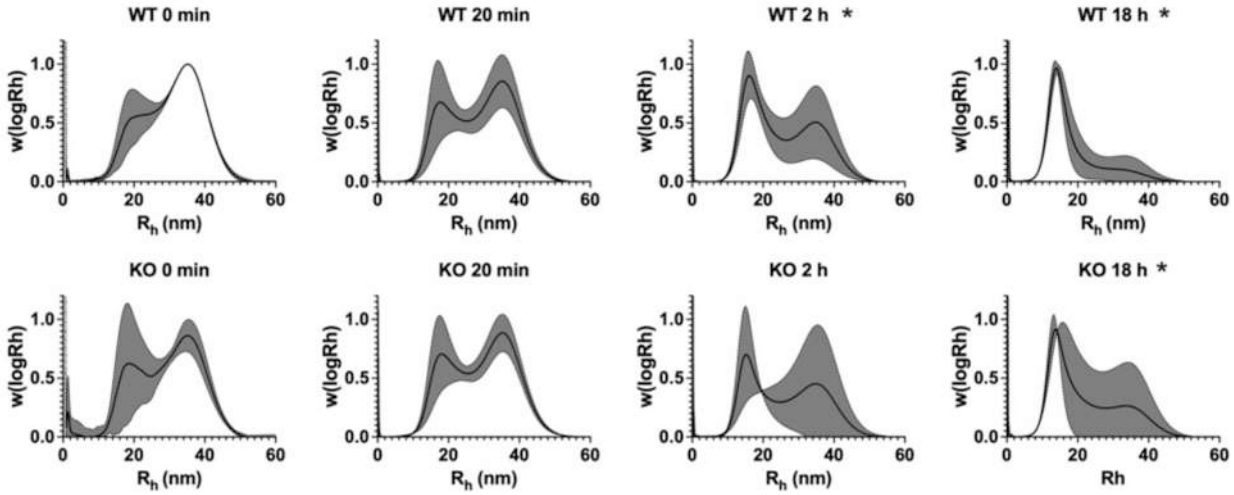

Fig. 6. SEC weight distribution of WT and Gyg KO (KO) mouse liver glycogen under acid degradation (pH = 3.5) over time. BetaRatio of treatment group showing significant difference compared to untreated group (0 min) is labelled with "*".

activity in the livers of WT and Gyg KO mice. Hepatic GS and GP activity showed no significant difference between the two genotypes (Fig. 7A, B, C, and D). Moreover, WT and Gyg KO mice showed similar GS and GP protein levels (Fig. 7E and F).

The hepatic energy state is defined by adenine nucleotide levels, particularly by the AMP/ATP ratio [24]. It has been suggested that liver glycogen contributes to decreasing appetite by maintaining hepatic ATP levels during fasting [23,42]. To analyze the energy state of the livers of WT and Gyg KO mice, the amounts of ATP, AMP and ADP were measured. No significant differences between the two genotypes were observed (Fig. 8A, B and C).

3.6. *Glycogen re-synthesis after fasting*

To analyze the capacity of WT and Gyg KO mice to re-synthesize liver glycogen after depletion, the animals were fasted for 16 h and injected

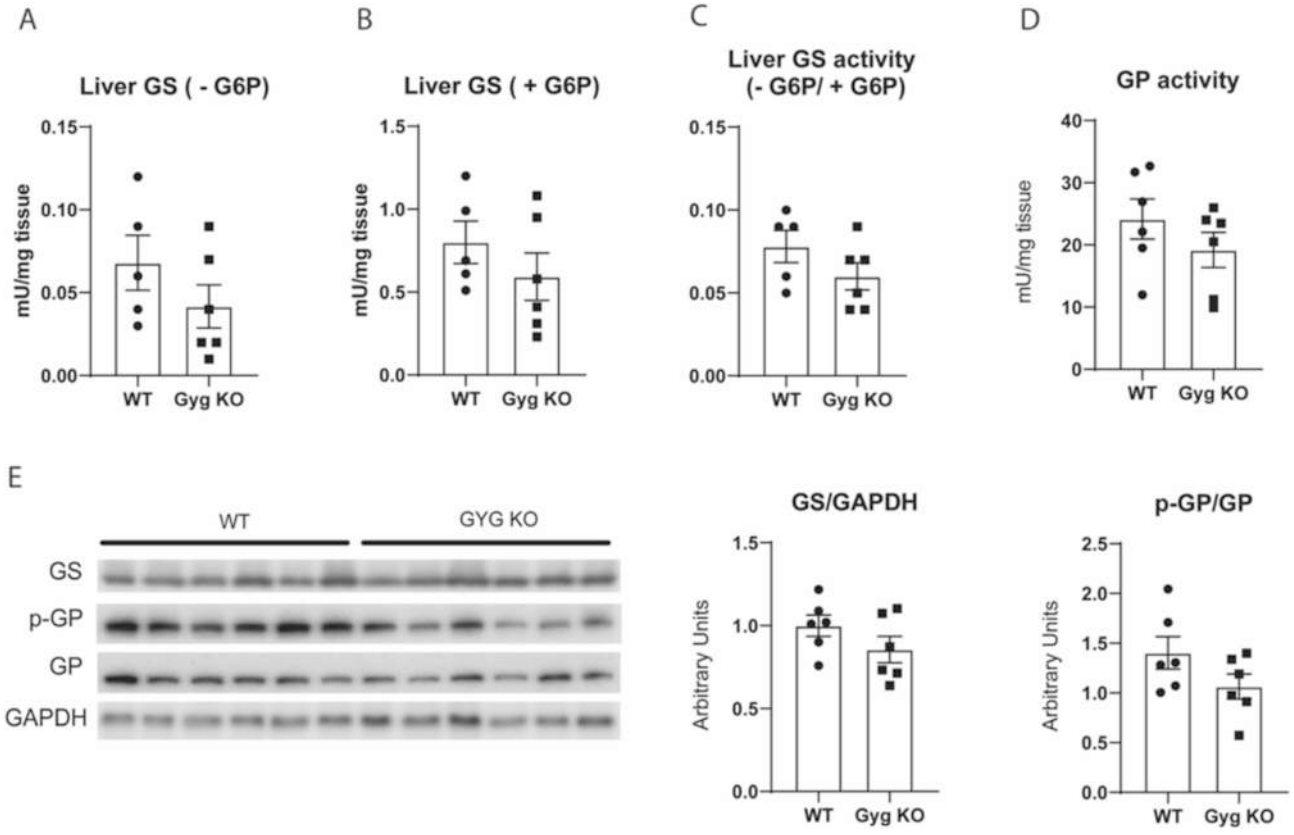

Fig. 7. Biochemical characterization of key enzymes related to glycogen metabolism. A) Enzymatic activity of liver GS in the absence of G6P, corresponding to the active GS form; $n = 5–6$ per group. B) Enzymatic activity of liver GS in the presence of G6P, corresponding to the total amount of GS; n = 5–6 per group. C) Activity ratio (ratio -G6P/+G6P); n = 5–6 per group. D) Enzymatic activity of liver GP in the presence of AMP; $n = 6$ per group. E) Immunoblot for GS, phosphorylated GP (p-GP), GP and GAPDH (as a loading control) in the livers of WT and Gyg KO mice, and quantification of the western blots; n = 6 per group.

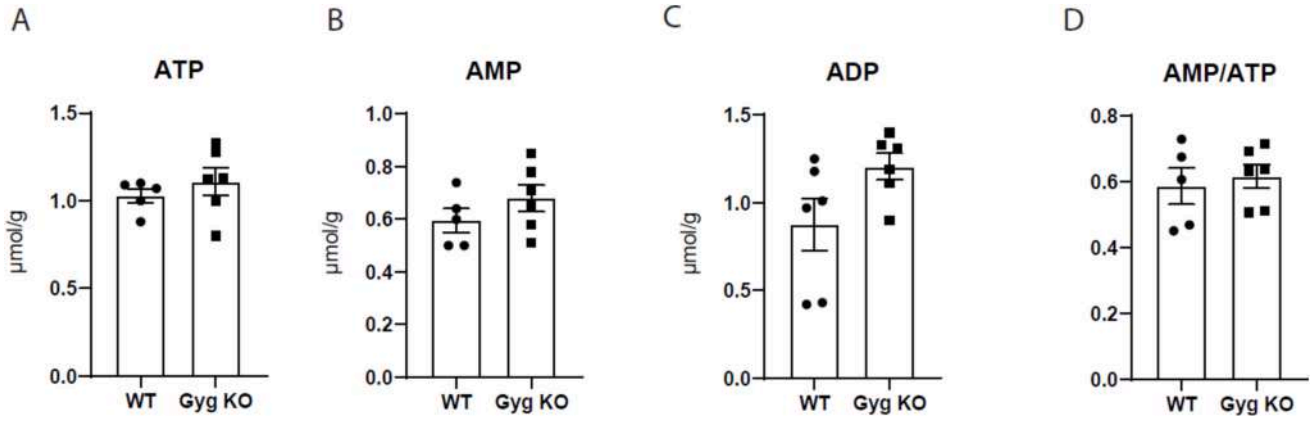

Fig. 8. Liver nucleotides in WT and Gyg KO mice. A) ATP levels. B) AMP. C) ADP levels. D) AMP/ATP ratio. n = 5–6 per group.

intraperitoneally with glucose. Liver glycogen was then measured at several time points post-injection. Glycogen content in WT livers showed a dramatic decrease after fasting, as previously described [19,20,23,25,26,42]. This decrease was slightly but significantly smaller in Gyg KO livers (Fig. 9A). Thirty minutes after glucose injection, glycogen content was also slightly but significantly higher in the livers of Gyg KO mice than in those of controls. However, 60 min after the injection, there was no significant difference between the two groups (Fig. 9A). We next measured liver GS activity in the two genotypes. The only significant difference was found 60 min after glucose injection, when WT mice showed higher GS activity (–G6P) and a higher –G6P/+G6P activity ratio (Fig. 9B and D). No significant differences in total GS activity (+G6P) were found between the two genotypes (Fig. 9C).

3.7. Liver metabolites

We next measured metabolites related to carbohydrate metabolism in the livers of WT and Gyg KO mice under fed conditions, fasted conditions, and 30 or 60 min after glucose administration. WT and Gyg KO livers showed similar levels of lactate (Fig. 10A), G6P (Fig. 10B), ATP (Fig. 10C) and triglycerides (TG) under all conditions (Fig. 10D).

3.8. Glycemic control

The increase in muscle glycogen in Gyg KO mice has been reported to be accompanied by muscle function impairment [10]. This observation was limited to muscle, which involves a different carbohydrate metabolism compared to the liver, which is the other main glycogen-storage tissue in mammals [43]. Liver glycogen is mobilized to generate glucose, which is released into the blood to maintain whole-body glucose homeostasis, while muscle glycogen is used mainly as a local energy supply during muscle fiber contraction [44]. Although glycogen levels were normal in the livers of Gyg KO mice, we examined whether glycemic control was altered in these animals. Glycaemia characterization was conducted in WT and Gyg KO and control mice, including glucose-level monitoring after long fasting (Fig. 11A), a glucose tolerance test (Fig. 11B), an insulin tolerance test (Fig. 11C) and a glucagon tolerance test (Fig. 11D). In all these experiments, Gyg KO mice showed no significant differences compared to WT mice, indicating that glycemic control is not altered in the absence of glycogenin.

4. Discussion

The biochemical function of glycogenin has been well established regarding self-glycosylation [9], the initiation of glycogen synthesis [45], and as a primer for the latter [46]. Due to these well-recognized biological roles, glycogenin had been regarded as essential for glycogen metabolism, an inference supported by clinical cases where glycogenin deficiency was associated with glycogen synthesis defects [47–49]. However, recent studies have demonstrated that glycogenin is in fact dispensable for glycogen synthesis. First, we reported that Gyg KO mice accumulate glycogen in multiple tissues, including skeletal muscle, liver, and others [10,12]. Furthermore, glycogen is present in human muscle tissue from patients lacking both GYG1 and GYG2 [11]. Despite glycogenin not being essential for glycogen synthesis, its significant role in glycogen metabolism raises intriguing questions. Indeed, glycogenin must have important roles that justify its widespread conservation across numerous species. In this regard, the skeletal muscle of Gyg KO mice accumulates four times more glycogen than that of WT litter mates [10], thereby indicating that the synthesis of glycogen, while possible, is deregulated in the absence of glycogenin in this tissue.

Although glycogen is present at normal levels in the livers of Gyg KO mice in fed conditions [10], here we explored whether the absence of glycogenin also interferes with normal liver glycogen metabolism. In this regard, glycogenin was proposed as a potential linking agent of glycogen β particles to form α particles [18], noting, as pointed out above, that this linking agent does not have to be the same in all organisms. The formation of α particles in the liver is important for correct regulation of glycaemia, as these particles degrade more slowly than β-type ones, enabling the controlled release of blood glucose [17]. Thus, here we tested the hypothesis that the lack of glycogenin in mouse liver would lead to a decrease or the absence of glycogen α particles, thereby impacting mouse-liver metabolism and whole-body glucose homeostasis.

Our results did not support this hypothesis. First, in a proteomic study, only some proteins related to fatty acid synthesis or ATP production were significantly different. However, no GO terms were significantly enriched from the list of differentially abundant proteins, thus indicating that the livers of Gyg KO mice do not substantially differ from those of WT animals. Regarding the characterization of glycogen structure, the distribution of molecular size and chain lengths were very similar in glycogen obtained from WT and Gyg KO livers. These results suggest that the absence of glycogenin does not affect glycogen α-particle formation. However, to find possible subtle differences in α-particle formation or stability, we studied degradation patterns under acid conditions. In this regard, α particles in diabetic mice are easily broken down into β particles, which impacts glycemic control [17]. Again, we did not observe any significant difference when the acid-degradation pattern of Gyg KO liver glycogen was compared to that of WT mice.

In line with the lack of changes in glycogen structure, Gyg KO liver glycogen metabolism was very similar to that of WT livers. While it would be of interest to conduct metabolomic analysis of Gyg KO and WT mice livers, this is not needed to test our hypothesis about glycogen structure and glucose metabolism requires targeted characterization of glycogen- related enzyme activity, energy state and levels of key metabolites. For this, we applied targeted biochemical characterization

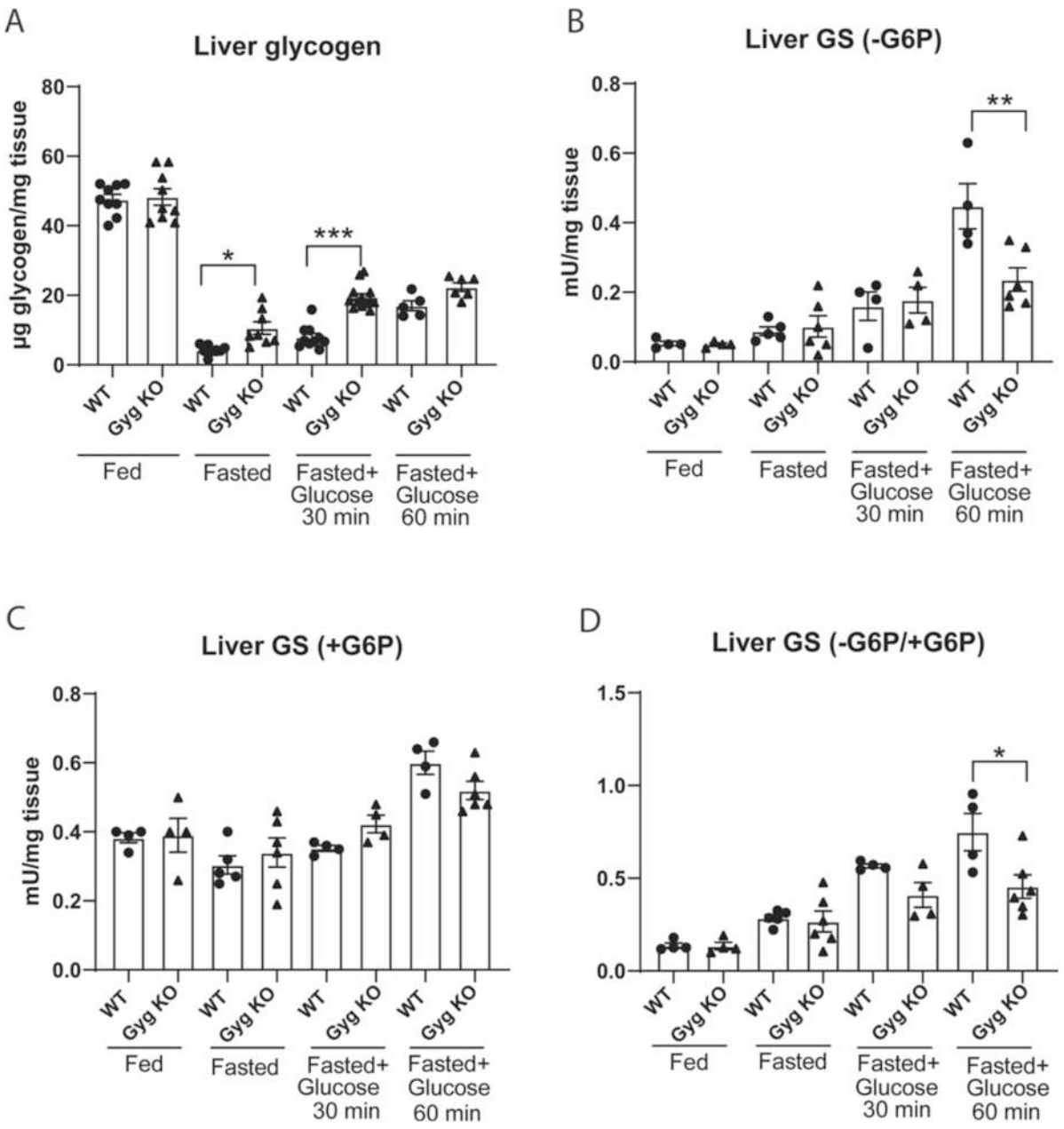

Fig. 9. Glycogen re-synthesis and liver GS characterization. A) Glycogen levels after bolus glucose injection in Gyg KO and WT mice. Gyg KO mice were fasted for 16 h, followed by intraperitoneal administration of glucose (2 mg/g body weight). Mice were sacrificed at the indicated time points and liver glycogen levels were determined ($n = 5$–13 per group). B) Glycogen synthase activity (–G6P) after bolus glucose injection in Gyg KO and WT mice. Gyg KO mice were fasted for 16 h, followed by intraperitoneal administration of glucose (2 mg/g body weight). Mice were sacrificed at the indicated time points and liver glycogen levels were determined ($n = 4$–6 per group). C) Glycogen synthase activity (+G6P) after bolus glucose injection in Gyg KO and WT mice. Gyg KO mice were fasted for 16 h, followed by intraperitoneal administration of glucose (2 mg/g body weight). Mice were sacrificed at the indicated time points and liver glycogen levels were determined ($n = 4$–6 per group). D) Glycogen synthase activity (–G6P/+G6P) after bolus glucose injection in Gyg KO and WT mice. Gyg KO mice were fasted for 16 h, followed by intraperitoneal administration of glucose (2 mg/g body weight). Mice were sacrificed at the indicated time points and liver glycogen levels were determined (n = 4–6 per group). *$p < 0.05$, **$p < 0.01$, ***$p < 0.001$.

(Figs. 7–11). Metabolomics can provide a more comprehensive characterization of potential features in biological samples. However, metabolomic analysis only provides semi-quantitative information and is best verified by targeted biochemical analysis, as we have done in the manuscript. Here, we have characterized enzymatic activity and quantitation of key proteins involving in glucose metabolism: GS and GP. This covers both key enzymes involved in the glycogen synthesis and degradation phases. No significant changes were found in the protein expression or activity of GS or GP, the two main enzymes responsible for glycogen synthesis and degradation, respectively. The hepatic energy state was very similar between the two genotypes, as measured by the amount of ATP, ADP, and AMP. Similarly, no changes were observed in liver metabolites such as lactate, G6P or TG. To further discard a difference in glycogen dynamics, we subjected WT and Gyg KO mice to overnight fasting to deplete liver glycogen, and we measured glycogen re-synthesis after intraperitoneal glucose injection. Gyg KO liver glycogen content was slightly higher in fasting conditions and 30 min after glucose infusion. However, 60 min after glucose injection, these differences disappeared, and glycogen levels became similar in WT and Gyg KO livers. In line with this, GS activity was slightly higher in Gyg KO

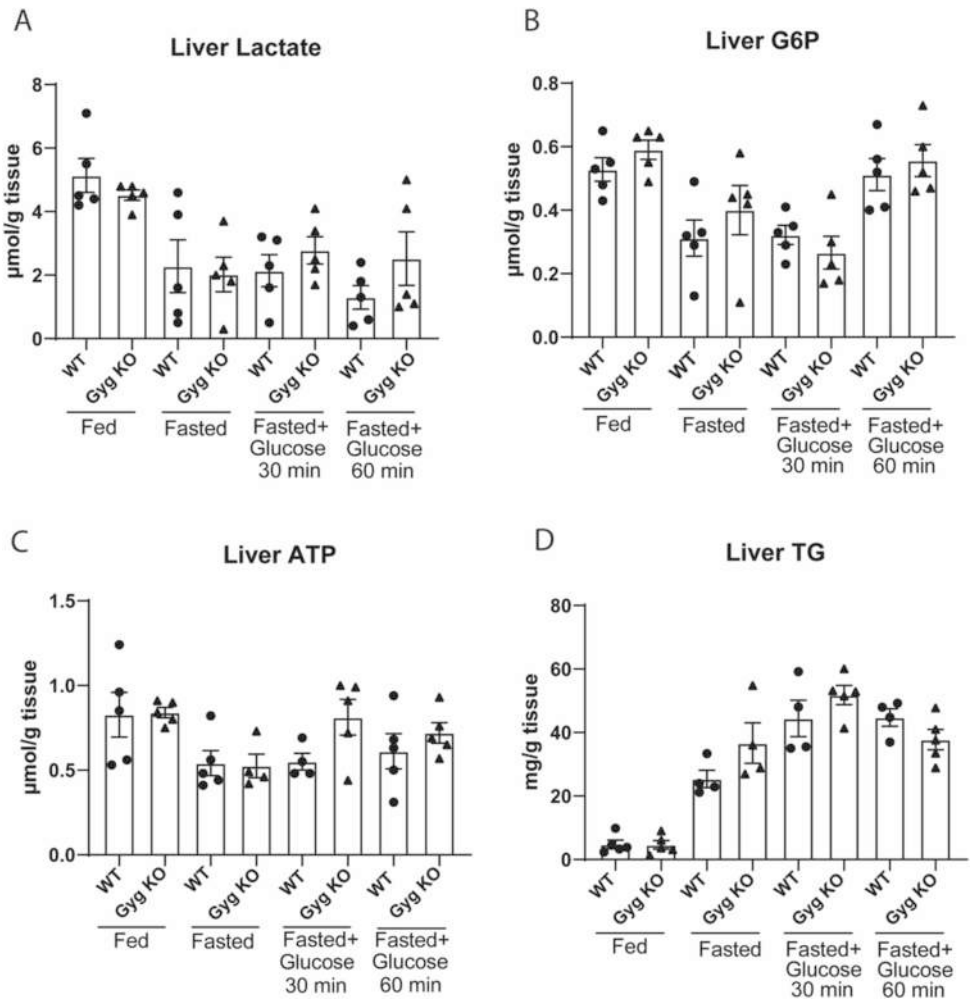

Fig. 10. Metabolic characterization for fed, fasted and after injection of glucose bolus. Mice were fasted for 16 h, followed by intraperitoneal administration of glucose (2 mg/g body weight), and sacrificed at the indicated times. A) Liver lactate levels ($n = 5$ per group). B) Liver G6P levels (n = 5 per group). C) Liver ATP (n = 4–5 per group). D) Liver TG levels (n = 4–5 per group).

livers 60 min after glucose injection. The underlying mechanisms for these kinetic differences in mouse-liver metabolism induced by the absence of glycogenin require further research. However, the levels of lactate, G6P, ATP and TG were similar in both groups in all conditions. Furthermore, these slight changes were only observed at the early stage of glycogen synthesis. This transient difference in the glycogen synthesis kinetics observed only in Gyg KO mice did not have an observable impact on whole-glucose body homeostasis. Indeed, blood glucose levels in fed and fasted conditions were similar in both genotypes. Along the same lines, the glucose tolerance test, insulin tolerance test and glucagon tolerance test showed no differences between genotypes. Taken together, these results indicate that the absence of glycogenin does not lead to altered glucose homeostasis.

This surprising result (that glycogen content, glycogen synthase, and glycogen phosphorylase activities were not significantly different in our wild-type vs. Gyg KO comparison) could be from more than one possibility. a) A compensatory mechanism exists to replace the glycogenin function in animal liver to initiate glycogen synthesis. A similar mechanism was proposed in yeast where hyperactive glycogen synthase was proposed to enhance glycogen synthesis at the absence of glycogenin [50]. b) Glycogenin has some novel function(s) beyond being the glycogen primer, which do(es) not alter glycogen synthase or glycogen phosphorylase activity or only affect(s) the activities transiently. In the other word, potential glycogenin novel function is associated with glycogen synthesis kinetics but not final glycogen structure or size. This possible novel function may be associated only with early glycogen synthesis. This possibility is partially supported in previous research where a glycogen synthase – glycogenin complex modulates glycogen synthesis through an avidity effect [48]. Also, a linking area in glycogenin was reported to associate with final glycogen size [51].

Our findings show that the current model for the formation of glycogen α particles and glucose metabolism, which highlights glycogenin as an essential component, is incomplete. The liver appears to maintain glucose metabolism and glycogen structure in the absence of glycogen α particles, indicating that alternative pathways in glycogen structure and glucose metabolism need to be explored.

5. Conclusions

This study showed that glycogenin is dispensable for normal liver glycogen metabolism and body glucose homeostasis. No significant differences were observed in the structure of glycogen in terms of chain length distribution and molar mass/size distributions of Gyg KO mice liver glycogen compared to that of WT mice. Glycogen structural analysis demonstrated that the linkage between glycogen β particles is unlikely to be driven by glycogenin, refuting what had been previously proposed. The absence of glycogenin resulted only in minor changes in glycogen content at the early stage of synthesis; however, these changes did not result in altered whole-body glucose homeostasis.

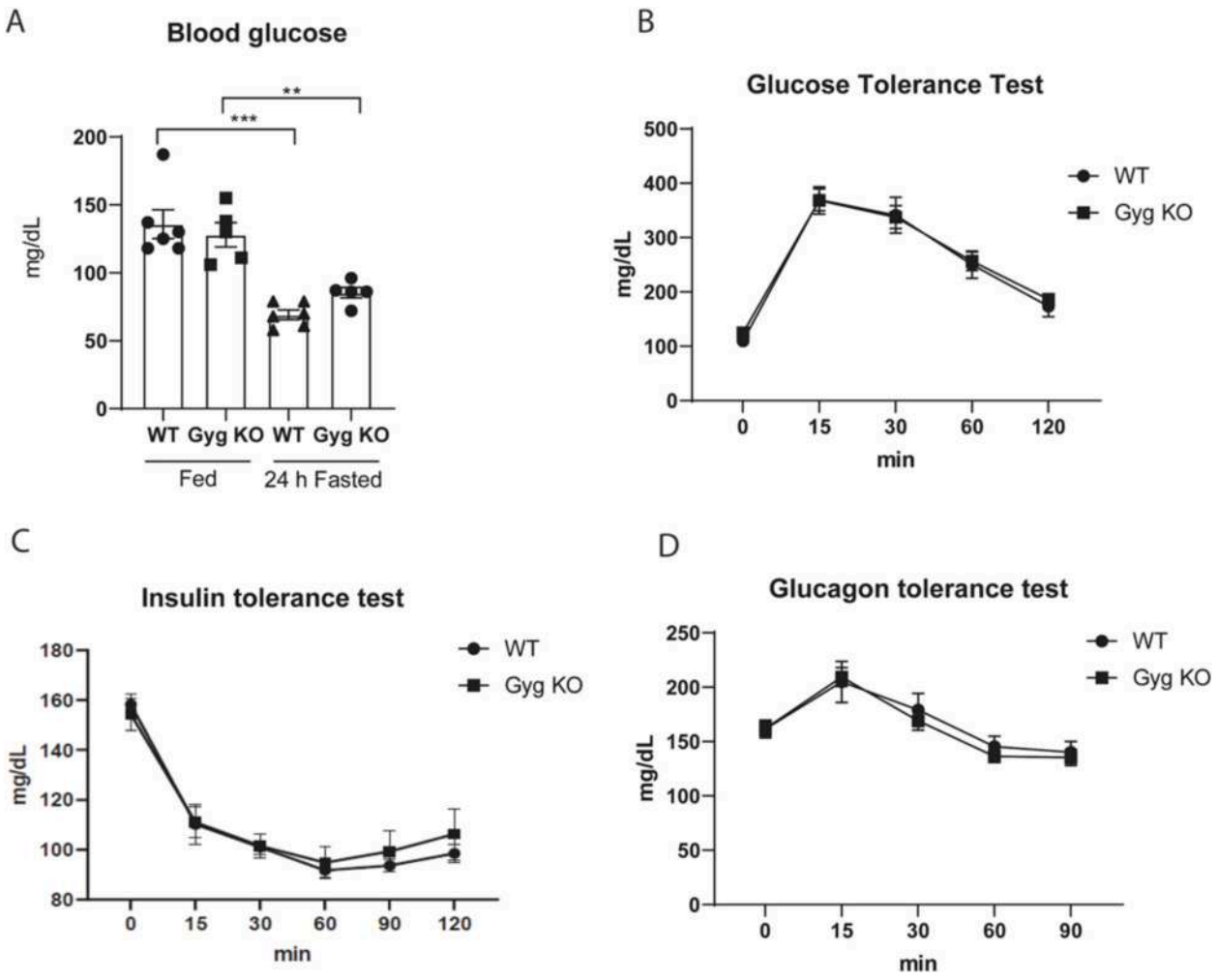

Fig. 11. Metabolic characterization of WT and Gyg KO mice. A) Blood glucose levels in fed and 24-h fasted WT and Gyg KO mice. n = 5–6 per group. B) Glucose tolerance test in WT and Gyg KO mice. $n = 8$–13 per group. C) Insulin tolerance test in WT and Gyg KO mice. $n = 6$–8 per group. D) Glucagon tolerance test in WT and Gyg KO mice. $n = 10$–17 per group. $^{**}p < 0.01$, $^{***}p < 0.001$.

CRediT authorship contribution statement

Xinle Tan: Writing – review & editing, Writing – original draft, Validation, Methodology, Investigation, Formal analysis, Data curation, Conceptualization. **Giorgia Testoni:** Writing – review & editing, Supervision, Methodology, Investigation, Formal analysis, Data curation. **Mitchell A. Sullivan:** Writing – review & editing, Supervision, Methodology, Investigation, Funding acquisition. **Iliana López-Soldado:** Writing – review & editing, Validation, Investigation. **Francisco Vilaplana:** Writing – review & editing, Investigation. **Robert G. Gilbert:** Writing – review & editing, Supervision, Resources, Project administration, Methodology, Investigation, Funding acquisition, Formal analysis. **Joan J. Guinovart:** Methodology, Formal analysis. **Benjamin L. Schulz:** Writing – review & editing, Validation, Resources, Methodology, Investigation, Formal analysis. **Jordi Duran:** Writing – review & editing, Supervision, Resources, Project administration, Methodology, Formal analysis.

Funding

This study was supported by a grant from the Spanish Ministry of Science, Innovation, and Universities (MCIU/FEDER/AEI) (PID2020-118699GB-I00 to JD), and a grant from the Fundación Ramón Areces to JD. Funding was also obtained from the National Natural Science Foundation of China (grant number C1304013151101138), and the Priority Academic Program of Jiangsu Higher Education Institutions to RGG.

Declaration of competing interest

The authors claim no competing interests.

Data availability

Data will be made available on request.

References

[1] G.F. Young, Claude Bernard and the discovery of glycogen, Br. Med. J. 1 (1957) 1431–1437.
[2] F.D. Calonge, The occurrence of glycogen-membrane complexes in fungi, An electron microscope study, Protoplasma 67 (1) (1969) 79–85.
[3] W.A. Wilson, P.J. Roach, M. Montero, E. Baroja-Fernández, F.J. Muñoz, G. Eydallin, A.M. Viale, J. Pozueta-Romero, Regulation of glycogen metabolism in yeast and bacteria, FEMS Microbiol. Rev. 34 (6) (2010) 952–985.
[4] L. Wang, Q. Liu, X. Tan, Z. Wang, M. Wang, M.J. Wise, C. Li, C. Ma, E. Li, B. Deng, Y. Du, D. Tang, R.G. Gilbert, Molecular structure of glycogen in Escherichia coli, Biomacromolecules 20 (7) (2019) 2821–2829.
[5] Y. Cao, A.V. Skurat, A.A. DePaoli-Roach, P.J. Roach, Initiation of glycogen synthesis. Control of glycogenin by glycogen phosphorylase, J. Biol. Chem. 268 (29) (1993) 21717–21721.
[6] P.J. Roach, A.V. Skurat, Self-Glucosylating initiator proteins and their role in glycogen biosynthesis, in: K. Moldave (Ed.), Progress in Nucleic Acid Research and Molecular Biology, Academic Press1997, pp. 289–316.

[7] J. Mu, A.V. Skurat, P.J. Roach, Glycogenin-2, a novel self-glucosylating protein involved in liver glycogen biosynthesis*, J. Biol. Chem. 272 (44) (1997) 27589–27597.
[8] L. Zhai, J. Schroeder, A.V. Skurat, P.J. Roach, Do rodents have a gene encoding glycogenin-2, the liver isoform of the self-glucosylating initiator of glycogen synthesis? IUBMB Life 51 (2) (2001) 87–91.
[9] A. Lin, J. Mu, J. Yang, P.J. Roach, Self-Glucosylation of Glycogenin, the initiator of glycogen biosynthesis, involves an inter-subunit reaction, Arch. Biochem. Biophys. 363 (1) (1999) 163–170.
[10] G. Testoni, J. Duran, M. García-Rocha, F. Vilaplana, A.L. Serrano, D. Sebastián, I. López-Soldado, M.A. Sullivan, F. Slebe, M. Vilaseca, P. Muñoz-Cánoves, J. J. Guinovart, Lack of Glycogenin causes glycogen accumulation and muscle function impairment, Cell Metab. 26 (1) (2017) 256–266.e4.
[11] K. Visuttijai, C. Hedberg-Oldfors, C. Thomsen, E. Glamuzina, C. Kornblum, G. Tasca, A. Hernandez-Lain, J. Sandstedt, G. Dellgren, P. Roach, A. Oldfors, Glycogenin is dispensable for glycogen synthesis in human muscle, and Glycogenin deficiency causes Polyglucosan storage, J. Clin. Endocrinol. Metab. 105 (2) (2020) 557–566.
[12] G. Testoni, B. Olmeda, J. Duran, E. López-Rodríguez, M. Aguilera, M.I. Hernández-Álvarez, N. Prats, J. Pérez-Gil, J.J. Guinovart, Pulmonary glycogen deficiency as a new potential cause of respiratory distress syndrome, Hum. Mol. Genet. 29 (21) (2020) 3554–3565.
[13] J. Shearer, T.E. Graham, Novel aspects of skeletal muscle glycogen and its regulation during rest and exercise, Exerc. Sport Sci. Rev. 32 (3) (2004) 120–126.
[14] R. Geddes, J.D. Harvey, P.R. Wills, The molecular size and shape of liver glycogen, Biochem. J. 163 (2) (1977) 201–209.
[15] X. Jiang, P. Zhang, S. Li, X. Tan, Z. Hu, B. Deng, K. Wang, C. Li, M.A. Sullivan, E. Li, R.G. Gilbert, Molecular-size dependence of glycogen enzymatic degradation and its importance for diabetes, Eur. Polym. J. 82 (2016) 175–180.
[16] Z. Hu, B. Deng, X. Tan, H. Gan, C. Li, S.S. Nada, M.A. Sullivan, J. Li, X. Jiang, E. Li, R.G. Gilbert, Diurnal changes of glycogen molecular structure in healthy and diabetic mice, Carbohydr. Polym. 185 (2018) 145–152.
[17] A. Nawaz, P. Zhang, E. Li, R.G. Gilbert, M.A. Sullivan, The importance of glycogen molecular structure for blood glucose control, iScience 24 (1) (2021) 101953.
[18] X. Tan, M.A. Sullivan, S.S. Nada, B. Deng, B.L. Schulz, R.G. Gilbert, Proteomic investigation of the binding agent between liver glycogen β particles, ACS Omega 3 (4) (2018) 3640–3645.
[19] I. López-Soldado, J.J. Guinovart, J. Duran, Active glycogen synthase in the liver prevents high-fat diet-induced glucose intolerance, decreases food intake, and lowers body weight, Int. J. Mol. Sci. 24 (3) (2023) 2574.
[20] I. López-Soldado, J.J. Guinovart, J. Duran, Hepatic overexpression of protein targeting to glycogen attenuates obesity and improves hyperglycemia in db/db mice, Front Endocrinol (Lausanne) 13 (2022) 969924.
[21] S. Ros, M. García-Rocha, J. Calbó, J.J. Guinovart, Restoration of hepatic glycogen deposition reduces hyperglycaemia, hyperphagia and gluconeogenic enzymes in a streptozotocin-induced model of diabetes in rats, Diabetologia 54 (10) (2011) 2639–2648.
[22] D.P. Gilboe, K.L. Larson, F.Q. Nuttall, Radioactive method for the assay of glycogen phosphorylases, Anal. Biochem. 47 (1) (1972) 20–27.
[23] I. López-Soldado, R. Fuentes-Romero, J. Duran, J.J. Guinovart, Effects of hepatic glycogen on food intake and glucose homeostasis are mediated by the vagus nerve in mice, Diabetologia 60 (6) (2017) 1076–1083.
[24] I. López-Soldado, A. Bertini, A. Adrover, J. Duran, J.J. Guinovart, Maintenance of liver glycogen during long-term fasting preserves energy state in mice, FEBS Lett. 594 (11) (2020) 1698–1710.
[25] I. López-Soldado, J.J. Guinovart, J. Duran, Increasing hepatic glycogen moderates the diabetic phenotype in insulin-deficient Akita mice, J. Biol. Chem. 296 (2021) 100498.
[26] I. López-Soldado, J.J. Guinovart, J. Duran, Increased liver glycogen levels enhance exercise capacity in mice, J. Biol. Chem. 297 (2) (2021) 100976.
[27] A. Zhu, R. Romero, H.R. Petty, An enzymatic fluorimetric assay for glucose-6-phosphate: application in an in vitro Warburg-like effect, Anal. Biochem. 388 (1) (2009) 97–101.
[28] D.M. Salmon, J.P. Flatt, Effect of dietary fat content on the incidence of obesity among ad libitum fed mice, Int. J. Obes. (Lond) 9 (6) (1985) 443–449.
[29] C. Enculescu, E.D. Kerr, K.Y.B. Yeo, G. Schenk, M.R.S. Fortes, B.L. Schulz, Proteomics reveals profound metabolic changes in the alcohol use disorder brain, ACS Chem. Nerosci. 10 (5) (2019) 2364–2373.
[30] Y. Xu, U.-M. Bailey, B.L. Schulz, Automated measurement of site-specific N-glycosylation occupancy with SWATH-MS, PROTEOMICS 15 (13) (2015) 2177–2186.
[31] E.D. Kerr, C.H. Caboche, C.L. Pegg, T.K. Phung, C. Gonzalez Viejo, S. Fuentes, M. T. Howes, K. Howell, B.L. Schulz, The post-translational modification landscape of commercial beers, Sci. Rep. 11 (1) (2021) 15890.
[32] S.K. Osama, E.D. Kerr, A.M. Yousif, T.K. Phung, A.M. Kelly, G.P. Fox, B.L. Schulz, Proteomics reveals commitment to germination in barley seeds is marked by loss of stress response proteins and mobilisation of nutrient reservoirs, J. Proteomics 242 (2021) 104221.
[33] E.D. Kerr, C.H. Caboche, B.L. Schulz, Posttranslational modifications drive protein stability to control the dynamic beer brewing proteome*[S], Mol. Cell. Proteomics 18 (9) (2019) 1721–1731.
[34] M. Choi, C.-Y. Chang, T. Clough, D. Broudy, T. Killeen, B. MacLean, O. Vitek, MSstats: an R package for statistical analysis of quantitative mass spectrometry-based proteomic experiments, Bioinformatics 30 (17) (2014) 2524–2526.
[35] E.D. Kerr, T.K. Phung, C.H. Caboche, G.P. Fox, G.J. Platz, B.L. Schulz, The intrinsic and regulated proteomes of barley seeds in response to fungal infection, Anal. Biochem. 580 (2019) 30–35.
[36] S. Falcon, R. Gentleman, Using GOstats to test gene lists for GO term association, Bioinformatics 23 (2) (2006) 257–258.
[37] Y. Perez-Riverol, J. Bai, C. Bandla, D. Garcia-Seisdedos, S. Hewapathirana, S. Kamatchinathan, D.J. Kundu, A. Prakash, A. Frericks-Zipper, M. Eisenacher, M. Walzer, S. Wang, A. Brazma, J.A. Vizcaino, The PRIDE database resources in 2022: a hub for mass spectrometry-based proteomics evidences, Nucleic Acids Res. 50 (D1) (2022) D543–D552.
[38] P.O. Powell, M.A. Sullivan, J.J. Sheehy, B.L. Schulz, F.J. Warren, R.G. Gilbert, Acid hydrolysis and molecular density of phytoglycogen and liver glycogen helps understand the bonding in glycogen alpha (composite) particles, PloS One 10 (3) (2015) e0121337.
[39] M.A. Sullivan, P.O. Powell, T. Witt, F. Vilaplana, E. Roura, R.G. Gilbert, Improving size-exclusion chromatography separation for glycogen, J. Chromatogr. A 1332 (2014) 21–29.
[40] B. Deng, M.A. Sullivan, A.C. Wu, J. Li, C. Chen, R.G. Gilbert, The mechanism for stopping chain and Total-molecule growth in complex branched polymers, Exemplified by Glycogen, Biomacromolecules 16 (6) (2015) 1870–1872.
[41] Y. Rousset, O. Ebenhoh, A. Raguin, Stochastic modelling of a three-dimensional glycogen granule synthesis and impact of the branching enzyme, PLoS Comput. Biol. 19 (5) (2023) e1010694.
[42] I. López-Soldado, D. Zafra, J. Duran, A. Adrover, J. Calbó, J.J. Guinovart, Liver Glycogen Reduces Food Intake and Attenuates Obesity in a High-Fat Diet–Fed Mouse Model, Diabetes 64(3) (2014) 796–807.
[43] K. Bhattacharya, Investigation and management of the hepatic glycogen storage diseases, Transl Pediatr 4 (3) (2015) 240–248.
[44] S. Kanungo, K. Wells, T. Tribett, A. El-Gharbawy, Glycogen metabolism and glycogen storage disorders, Ann Transl Med 6 (24) (2018) 474.
[45] W.J. Whelan, The initiation of glycogen synthesis, Bioessays 5 (3) (1986) 136–140.
[46] J. Pitcher, C. Smythe, P. Cohen, Glycogenin is the priming glucosyltransferase required for the initiation of glycogen biogenesis in rabbit skeletal muscle, Eur. J. Biochem. 176 (2) (1988) 391–395.
[47] A.R. Moslemi, C. Lindberg, J. Nilsson, H. Tajsharghi, B. Andersson, A. Oldfors, Glycogenin-1 deficiency and inactivated priming of glycogen synthesis, N. Engl. J. Med. 362 (13) (2010) 1203–1210.
[48] E. Zeqiraj, X. Tang, R.W. Hunter, M. García-Rocha, A. Judd, M. Deak, A. von Wilamowitz-Moellendorff, I. Kurinov, J.J. Guinovart, M. Tyers, K. Sakamoto, F. Sicheri, Structural basis for the recruitment of glycogen synthase by glycogenin, Proc. Natl. Acad. Sci. 111 (28) (2014) E2831–E2840.
[49] E. Malfatti, J. Nilsson, C. Hedberg-Oldfors, A. Hernandez-Lain, F. Michel, C. Dominguez-Gonzalez, G. Viennet, H.O. Akman, C. Kornblum, P. Van den Bergh, N.B. Romero, A.G. Engel, S. DiMauro, A. Oldfors, A new muscle glycogen storage disease associated with glycogenin-1 deficiency, Ann. Neurol. 76 (6) (2014) 891–898.
[50] M.J. Torija, M. Novo, A. Lemassu, W. Wilson, P.J. Roach, J. Francois, J.L. Parrou, Glycogen synthesis in the absence of glycogenin in the yeast Saccharomyces cerevisiae, FEBS Lett. 579 (18) (2005) 3999–4004.
[51] E. Zeqiraj, F. Sicheri, Getting a handle on glycogen synthase - its interaction with glycogenin, Mol. Aspects Med. 46 (2015) 63–69.